COMPREHENSIVE EVALUATION METHOD FOR PERMEATION MECHANISM OF ASPHALT REGENERATOR

Fuming LIU[1, *], Shun SHEN[2], Faqian ZHEN[3], Jiayuan PENG[4]

In order to study the effect of the comprehensive performance of asphalt regenerants on their permeation mechanism, a permeation sandwich model was designed and four types of regenerants (non-petroleum-based regenerants NRA and NRB, petroleum-based regenerants PR and bio-oil-based regenerants BR) were selected for incorporation. Fourier transform infrared spectroscopy (FTIR) was used to test the changes of peak value and peak area of each regenerant and bitumen. The research results show that the penetration degree change graphs after the addition of regenerant will present four types of graphs - concave graph, convex graph, ascending graph and waveform graph. At the initial stage of heating, the regenerant fuses and regenerates with the upper layer of aged asphalt to form a surface aged asphalt film, resulting in the initial phenomenon of reduced penetration in the concave graph and waveform graph; With the increase of asphalt aging, the peak area of ketone carbonyl and sulfoxide absorption peaks gradually increased, the peak area of alkyl stretching vibration absorption peak gradually decreased, and the peak area of alkyl bending vibration absorption peak also decreased, according to FTIR results show that the effect of regenerant is different, causing the alkyl stretching vibration and bending vibration index to increase differently, so the regeneration ability of regenerant (alkyl change index) is BR>NRB>PR>NRA; the influence trend of regenerant penetration ability and regeneration ability is not consistent, so the evaluation of penetration mechanism should Therefore, the evaluation of the permeation mechanism should consider the permeation effect and regeneration effect of the regenerant.

Keywords: road engineering, permeability mechanism, needle penetration, regeneration agent, Fourier transform infrared spectrum

1. Introduction

With the renovation of old roads in various regions of China, the supply of RAP materials has gradually increased, and the amount of RAP admixture has been required to be continuously improved in various regions. However, while increasing the amount of RAP material, it is also necessary to continuously improve the regeneration effect, resulting in a more refined evaluation of RAP grades and

[1] School of Civil and Architectural Engineering, Jiangxi University of Water Resources and Electric Power, Nanchang, China; e-mail: 895709056@qq.com.
[2] Jiangxi Ganbei Highway Survey and Design Institute, Jiujiang, China
[3] Jiangxi Yichun Highway Construction Group Co, Yichun, China
[4] Jiangxi Yichun Highway Construction Group Co, Yichun, China

higher requirements for the regeneration effect of the regenerant [1]. Therefore, for the increasing performance requirements of regenerants, the greater the demand for regenerants, the more research and development for regenerants, which contain polar ester carbonyl, hydroxyl, sulfoxide groups and non-polar methyl and methylene can play a different role [2]. According to the classification of raw materials used for the production of regenerants, there are studies on waste cooking oil, waste bio-oil and waste engine oil [3], among which waste engine oil has poor performance of recycled asphalt after secondary aging due to the presence of ash inside [4], waste bio-oil regenerants have poor high-temperature performance and good anti-aging properties [5], waste cooking oil is not widely used and its lighter components differ significantly from other molecular weights affecting The compatibility of components of recycled asphalt [6]; Chen et al. [7] found that bio-oil-based regenerants have relatively better recovery effect and outstanding anti-aging properties. Jain et al. [8] demonstrated that the addition of waste vegetable oil can effectively supplement the content of saturated hydrocarbons and aromatics and inhibit the oxidation of saturated hydrocarbons and aromatics to asphaltenes and resins. According to the classification of the developed regenerant properties, there are studies on sensitive regenerants, permeable regenerants and high permeability regenerants, etc. Sensitive regenerants are more effective in regenerating lightly aged old asphalt and less effective in regenerating heavily aged old asphalt [9], permeable regenerants show good activation effect and can improve the bonding at the regeneration interface [10], high permeability regenerants are effective in regenerating lightly aged asphalt through component modifiers, The effect of high permeability regenerants is more significant than that of ordinary regenerants through the addition of component modifiers, permeating agents and lightweight components [11].

The three regeneration mechanism theories generally agreed by scholars are "component regulation theory" [12], "compatibility theory" [13] and "surface wetting theory". Component regulation relies on the addition of certain components to make the components coordinate to achieve regeneration effect [14], compatibility regenerates by adjusting the solubility parameter between components, and surface wetting mainly achieves regeneration effect through uniform and rapid penetration of interface [15]. Chen et al. [16] used droplet morphology analyzer and DSR to analyze the degree of fusion concluded that regenerants are more likely to occur on the surface of short-term aged waste asphalt by spreading wetting action film formation and diffusion fusion reaction. To further analyze the recycled asphalt, most scholars verify the stability of recycled asphalt by secondary aging [17]. The aging methods usually use UV aging, RTFOT short-term aging and PAV aging. Wang and Zhang [18] used BBR and GPC tests to analyze the low temperature performance and aging nature of different aging methods to conclude that the regeneration process of asphalt is not exactly the aging

process a reverse process. Elkashef et al. [19] used scanning calorimetric analysis (MDSC) and low temperature infrared spectroscopy (LT-FTIR) to analyze the thermal reversible aging mechanism of different aging methods of regenerated asphalt to conclude that thermal reversible aging is not an inherent property.

With the support of the theory, the feasibility of the diffusion [20], penetration and fusion of the regenerant in the aged asphalt was then verified [21]. When the regenerant is added, it is required that the regenerant has good penetration into the asphalt and can diffuse uniformly, and the penetration and diffusion of the regenerant can be explained as the transfer of substances due to random molecular Brownian motion [22-23]. Zhan et al. [24] used needle penetration and DSR tests to verify the rutting factor analysis of three different components of asphalt to verify the diffusion uniformity. Forton et al. [25] calculated the steady-state shear viscosity of various binders based on the results of the complex modulus test and investigated the relationship between the steady-state shear viscosity and the penetration coefficient. The main test methods for the diffusion, permeation and fusion of regenerants are the "needle penetration method" and the "test tube method". The advantage of the needle penetration method is that the permeation process can be characterized in real time, but the operation is tedious. Xu et al. [26] used BBR and DSR tests to examine the diffusion performance of the test tube method for each layer of asphalt and concluded that a high content of small molecules is more effective for the regeneration of aged asphalt. Cui [27] used FTIR to analyze the carbonyl index, sulfoxide index and aromatic index of the two diffusion tests of needle penetration and test tube method and then derived the regeneration mechanism and diffusion mechanism of aged asphalt. At present, the study of regenerant diffusion mechanism is still in the detection of the optimal amount of regenerant doping, the effect on the generation of functional groups, or a one-sided study of the penetration of regeneration and not more intuitive data to evaluate the penetration and regeneration ability of regenerant. In view of this, this study is based on the test method of asphalt needle penetration for each group of samples of the permeable sandwich model to indirectly respond to the strength of the permeation performance of the regenerant and analyze the changes of functional groups by Fourier infrared spectroscopy (FTIR) and the changes of peak area using OMSNIC software to verify the regeneration effect of regenerated asphalt.

2. Raw material performance analysis

2.1 Substrate asphalt

The substrate asphalt used is Guangdong Maoming 70 A road petroleum asphalt, the asphalt indicators in line with the "Technical Specification for Highway Asphalt Pavement Construction" (JTG F40-2004) its technical indicators are shown in Table 1.

Table 1

Base asphalt performance index

Index		Unit	Test results	Code requirement
Degree of penetration (25℃)		0.1mm	72	60~80
Softening point		℃	54	≥46
The needle penetration index PI		--	-0.92	-1.5~+1.0
10 ℃ degree		cm	24.3	≥20
15 ℃ degree		cm	＞100	≥100
Density		g/cm³	1.027	Measured
Film or rotated film after heating	The quality change	%	0.14	-0.8~0.8
	Residual needle penetration ratio	%	70	≥61
	Residual elongation 10℃	cm	7.9	≥6
	Residual elongation 15℃	cm	28.3	≥15
	Dynamic viscosity at 60℃	Pa·s	195	≥180
Solubility		%	99.8	99.5
Flash point		℃	285	260

2.2 Aging asphalt

The aging asphalt used is Guangdong Maoming 70 A road petroleum asphalt by rotating film oven test RTFOT (85 min), and the use of PAV aging tester, take part of the RTFOT aging asphalt were PAV aging 20 h, 40 h test. The technical index of aging asphalt is shown in Table 2.

Table 2

Aging asphalt performance indicators

Material	Index	Unit	Test results
RTFOT aging asphalt	Degree of penetration (25℃)	0.1mm	40.7
	Softening point	℃	55.1
	15 ℃ degree	cm	32.7
PAV (20 h) aging asphalt	Degree of penetration (25℃)	0.1mm	27.9
	Softening point	℃	56.8
	15 ℃ degree	cm	20.7
PAV (40 h) aging asphalt	Degree of penetration (25℃)	0.1mm	14
	Softening point	℃	58.6
	15 ℃ degree	cm	7.6

2.3 Regenerant

Non-petroleum-based regenerant A (NRA) and non-petroleum-based regenerant B (NRB) were used. The main raw materials of the two non-petroleum-based regenerants were gutter oil, as well as commercially available petroleum-based regenerant C (PR) and bio-oil-based regenerant D (BR), as shown in Fig. 1. The technical specifications of each regenerant are shown in Table 3.

Table 3

Regenerating agent performance index

Index	Test results				Code requirement
	NRA	NRB	PR	BR	
Appearance	Yellow viscous liquid	Yellowish-black viscous liquid	Greenish-black viscous liquid	Black viscous liquid	\

Viscosity (60℃)/ (mm²/S)	53.6	98.6	207	251	50~900
Flash point/ (℃)	226	241	259	265	≥220
Saturation points/ (%)	28.9	14.3	25.6	12.9	≤30
Density (25℃)/ (g/cm²)	0.91	0.93	0.97	1.02	Measured
Film oven test viscosity ratio	1.52	1.51	1.13	1.47	≤3
Mass change/ (%)	-1.39	-0.42	-1.06	-0.72	≤4
Aromatic/(%)	54.9	42	42.3	52.4	Measured
Saturated/(%)	28.9	14.3	25.6	12.9	Measured
Asphaltene/ (%)	10.5	17.1	8.4	28.8	Measured
Gelatin/(%)	5.7	26.6	23.7	5.9	Measured

3. Analysis of test principles

3.1 Constructing an infiltration sandwich model

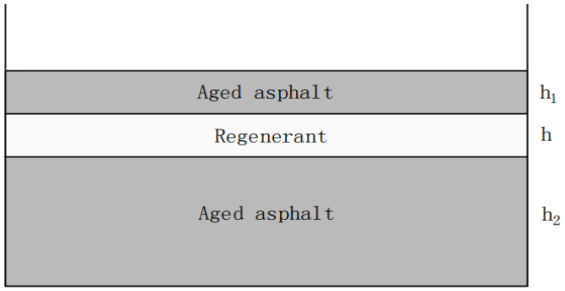

Fig. 1. Schematic Diagram of Permeable Interlayer Model

Fig. 2. PAV Pressure Aging Tester

The interlayer model designed in this paper is based on the mechanical structure and construction process of plant-mixed hot regeneration. From the perspective of exploring the penetration mechanism of the regenerant, a three-layer model that meets the practical application requirements has been constructed. In order to fully simulate the interlayer state of the regenerant and aged asphalt after adding the regenerant during the mixing process with the continuous mixing of the old and new materials in the mixing cylinder. A three-layer model of upper layer of

aged asphalt (height h1) - middle layer of regenerant (height h) - lower layer of aged asphalt (height h2) is constructed, as shown in Fig. 1. There are special requirements for the height h1 and h2 of the upper and lower layers of aged asphalt, and the needle penetration hr of the aged asphalt should be measured first, and the model should be constructed to ensure that h1≤hr and h2>hr. The safety of the instrument. In the process of making the model, it is necessary to ensure that each layer of the model is uniform and flat, and to ensure that h1 and h2 of each model are equal. In this study, the dosing of regenerant was 5 % and 10 %, and the size of h varied according to the dosing of regenerant. The models were kept in ovens at different temperatures and the penetration performance of the regenerant was characterized by testing the needle penetration of the models at different holding times.

3.2 Analysis of test methods

3.2.1 Needle penetration test

First of all, the needle penetration hr of RTFOT asphalt is measured, then the diameter d of the needle penetration dish and the total RTFOT asphalt height h are measured by vernier calipers to calculate the volume and weigh the total mass of asphalt in the needle penetration dish, and finally the ratio of height (h_r/h) can be obtained by adding the mass of RTFOT asphalt of height h_1, and calculating the mass of 5 % and 10 % to mix the regenerant but to ensure that $h_1 \leq h_r$ and $h_2 > h_r$.

After making the penetration sandwich model, it was cooled sufficiently for more than 1 h before conducting the subsequent needle penetration test. The model was heated in an oven at 110 ℃, 120 ℃, 130 ℃ and 140 ℃ for 1 h, 2 h, 3 h and 4 h respectively, then cooled at room temperature for 1 h and then placed in a water bath at 25 ℃ for 1.5 h. After the water bath was completed, the depth of the standard cone penetrating vertically into the asphalt specimen under a load of 100 g was measured as the needle penetration in 1/10 mm within 5 seconds. The test result is the average of three measurements.

3.2.2 PAV pressure aging test

The rotary film aging (RTFOT) asphalt was first made with No. 70 matrix asphalt, and then the RTFOT asphalt was passed through the PRENTEX-type PAV aging test apparatus, as shown in Fig. 2. PAV (20 h) and PAV (40 h) aging asphalt were prepared. the test parameters selected for PAV were: temperature: 100 ℃; pressure: 2.1 MPa; time: 20 h/40 h.

3.2.3 FTIR test

The NICOLET is10 infrared spectrometer was used for the test, with a scan range of 4000 to 400 cm-1 and a test detection cycle number of 32 bits (64 bits for the background), as shown in Fig. 3. The infrared spectra derived from the test were quantified by using OMSNIC software for peak and peak area analysis. The RTFOT asphalt with 5 % doping of the four regenerants was sheared by a high-speed shear,

and after shearing, it was put into a secondary aging oven at 130 ℃ for 4 h. After the end of the test, the samples were subjected to IR spectra. Adequate amounts of anhydrous ethanol, trichloroethylene and cotton balls were prepared for the test.

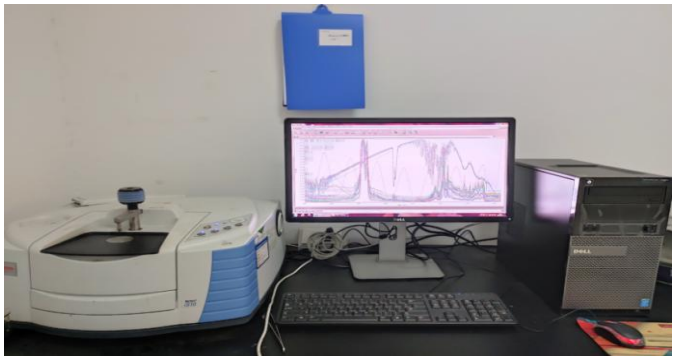

Fig. 3. Fourier Infrared Spectrometer

4.Test results and analysis

4.1 Needle penetration test results and analysis

From the test measured RTFOT asphalt needle penetration of 4.07 mm, vernier calipers measured the diameter of the needle penetration dish d = 52.67 mm, the total height of asphalt h = 32.70 mm, the measured mass m = 104.41 g, calculated by the formula h1 height of asphalt mass taken 13 g. In order to simplify the test to take h2 height at the mass of 37 g, that is, the regenerant dose of 5 % added 2.5 g, 10 % added 5 g. The above design all meet the requirements of h1≤hr, h2>hr. Needle penetration tests were conducted for models with different heating time, temperature, regenerant type and doping amount, and the results are shown in Fig. 4 and 5.

The graphs of needle penetration data in Fig. 4 and 5 can be summarized into four types, namely: concave graph (Fig. 4 (a) NRB) - The penetration degree first decreases and then increases over time; convex graph (Fig. 4 (d) NRB) - the penetration degree first increases and then decreases over time; ascending graph (Fig. 5 (a) NRA) - the penetration degree gradually increases over time; and waveform graph (Fig. 5 (b) NRA) - the penetration degree gradually fluctuates up and down over time.The main reason for the appearance of the concave graph is that the surface aging asphalt film formed after the regeneration of the regenerant and the upper layer of asphalt hinders the test from proceeding, so that the needle penetration decreases, but the subsequent continued heating and the continued penetration of the regenerant cause the needle penetration to continue to rise. The convex Fig. appears mainly in the sufficiently high temperature heating, regenerant continued penetration, needle penetration rose, with the extension of the heating time, the regenerant can not play a regeneration effect of penetration asphalt began to aging resulting in needle penetration decreased. The rising graph is mainly

temperature and regenerant continues to play a role. Waveform graph appears in the case of concave graph on the basis of continued heating regeneration asphalt aging phenomenon.

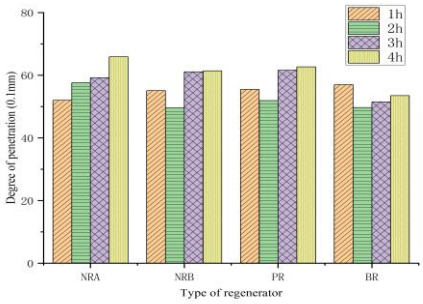

(a) Temperature 110 ℃, regenerating agent dosage 5%

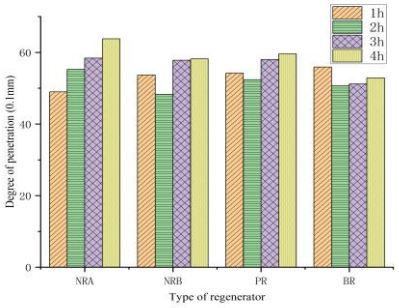

(b) Temperature 120 ℃, regenerating agent dosage 5%

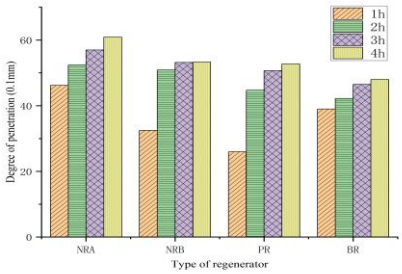

(c) Temperature 130 ℃, regenerating agent dosage 5%

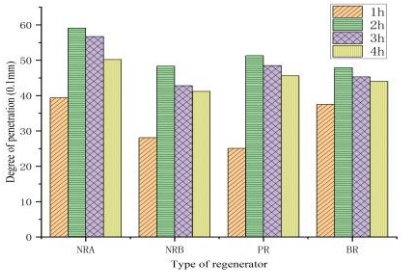

(d) Temperature 140 ℃, regenerating agent dosage 5%

Fig. 4. Effect of different temperature, time and regenerant type on regenerant penetration

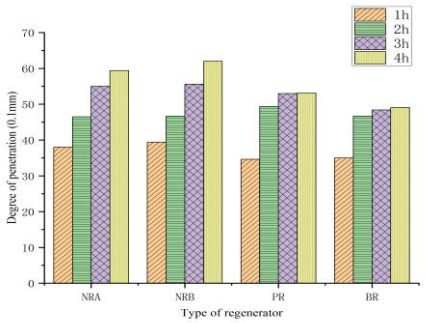

(a) Temperature 130 ℃, regenerating agent dosage 10%

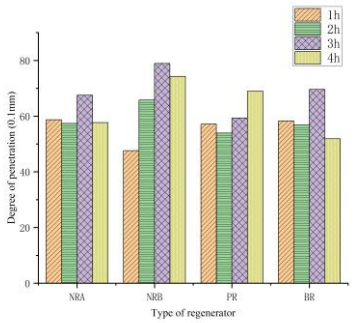

(b) Temperature 140 ℃, regenerating agent dosage 10%

Fig. 5. Effect of different regenerant dosing on regenerant penetration

As it can be seen from Fig. 4, with the heating temperature from 110 ℃ to 140 ℃, the penetration model needle penetration data graph of four different regenerants gradually changed from concave graph → rising graph → convex graph. The temperature change from 120 ℃ to 130 ℃ can be seen in the early

appearance of the surface aging asphalt film thus entering the process of downward penetration of the regenerant. However, from 130 ℃ to 140 ℃, all the regenerated permeable asphalt appeared aging phenomenon. With the heating time from 1 h to 4 h, the state in the infiltration model from the beginning of the formation of surface aging asphalt film to the disappearance of the asphalt film, while the regenerant continues to penetrate down the regeneration, and finally the end of the gradual aging process. In the penetration model test with the regenerant dose of 5 % at a heating temperature of 130 ℃ (Fig. 4(c)), it can be seen that the penetration effect of the regenerant is NRA > NRB > PR > BR.

From Fig. 5(a), it can be seen that with the increase of regenerant doping from 5 % to 10 %, the permeation model needle penetration of NRB, PR and BR increased by 16.3 %, 0.7 % and 2.3 %, respectively, but the NRA decreased by 2.5 %. The subsequent increase in the amount of regenerant not only cannot play a penetration effect but also has a resistance effect on the measurement of the penetration test, resulting in a slight decrease in the results. As can be seen from Fig. 5(b), 10 % of the regenerant penetration model at 140 ℃, the NRA and BR models both appear waveform data, which indicates that 140 ℃ and 10 % of the regenerant dosing with the initial appearance of the surface aging asphalt film phenomenon, but due to the high temperature of thermal aging, resulting in the penetration model from the appearance of the asphalt film to disappear immediately after the penetration process into the asphalt aging process. For NRB, although the model needle penetration test also entered the convexity diagram, but the regeneration penetration needle penetration increased by 27.3 %, which indicates that the optimal amount of NRB doping is around 10 %. For PR, the penetration model is still in the process from the appearance of the asphalt film to its disappearance and accompanying penetration, and the regenerative penetration needle penetration increased by 29.9 %, which indicates that the high temperature stability performance of PR is better.

4.2 FTIR test results and analysis

4.2.1 FTIR diagram of four regenerating agents

The FTIR spectra of the four regenerants are shown in Fig. 6. The peaks exhibited by the NRA in the IR spectra spectrum can be seen as follows: the -CH2- telescopic vibrational absorption peaks represented by alkyl groups at 2924.04 cm^{-1}, 2853.75 cm^{-1} and the bending vibrational absorption peaks of some single bonds (1464.59 cm^{-1}, 1377.27 cm^{-1}); carbonyl C═O stretching vibration absorption peaks in α-chlorinated non-cyclic ketones (1744.30 cm^{-1}) and in aliphatic ketones (1709.85 cm^{-1}) and C═C bond stretching and bending vibration absorption peaks in aliphatic ketones (1166.47 cm^{-1}); moderate to strong absorption peaks of long carbon chain saturated hydrocarbons -CH2- absorption peak (723.32 cm^{-1}) and the

vibrational absorption peak on the benzene ring (643.10 cm^{-1}), whose material consists mainly of light fractions of gutter oil and ketones.

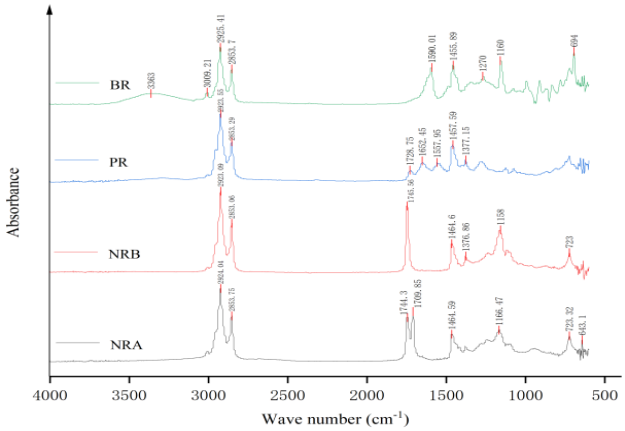

Fig. 6. FTIR Diagram of Four Regenerative Agents

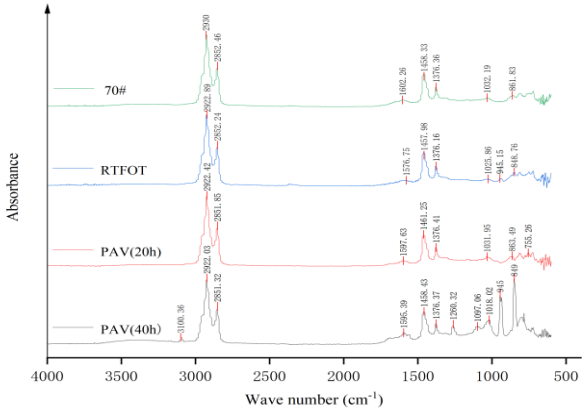

Fig. 7. FTIR Diagram Analysis of Aged Asphalt

The peaks exhibited by NRB in the IR spectra can be seen as follows: alkyl stretching vibrational absorption peaks at 2923.09 cm^{-1}, 2853.06 cm^{-1} and bending vibrational absorption peaks of some single bonds (1464.60 cm^{-1}, 1376.86 cm^{-1}); carbonyl C═O stretching vibrational absorption peaks in α-chlorinated acyclic ketones peak (1745.56 cm^{-1}) as well as the fingerprint region, which is mainly composed of light fractions of gutter oil, added asphaltene and gum fractions and ketones.

The peaks in the infrared spectra of PB can be seen as follows: -CH2- stretching vibration absorption peaks represented by alkyl groups at 2923.55 cm^{-1}, 2853.29 $cm^{-1}$and bending vibration absorption peaks of some single bonds (1457.59

cm^{-1}, 1377.15 cm^{-1}); carbonyl C═O (1728.75 cm^{-1}); the stretching vibration absorption peak of carbonyl C═O in the carboxylic acid anion (1652.45 cm^{-1}, 1557.95 cm^{-1}) and the fingerprint region, whose materials consist mainly of esters and carboxylic acids.

The peaks exhibited in the IR spectra of BR can be seen as follows: N-H stretching vibration absorption peaks in amines at 3363.00 cm^{-1} and C-H stretching vibration absorption peaks in aromatics at 3009.21 cm^{-1}; -CH2- stretching vibration absorption peaks represented by alkyl groups (2925.41 cm^{-1}). absorption peaks (2925.41 cm^{-1}, 2853.70 cm^{-1}) and bending vibration absorption peaks of some single bonds (1455.89 cm^{-1}); N-H bending vibration absorption peaks in ammonium salts (1590.01 cm^{-1}) and fingerprint regions, whose materials are mainly composed of amines.

The spectral analysis of the four regenerants shows that all four regenerants contain alkyl forms, and both NRA and NRB are made of gutter oil as the carrier and contain ketones, the only difference is that NRB adds a gum component to NRA, which reduces the viscosity of the regenerant and changes the regeneration performance. contains a large number of carbonyl compounds, while BR is characterized by amine compounds.

4.2.2 FTIR diagram analysis of aging asphalt

As shown in Fig. 7, the infrared spectrograms were analyzed by aging asphalt of matrix 70, RTFOT (85 min), and PAV aging for 20 h and 40 h. The alkyl telescopic vibrational absorption peaks (2923.00 cm^{-1}, 2852.46 cm^{-1}) and bending vibrational absorption peaks (1458.33 cm^{-1}, 1376.36 cm^{-1}) of matrix 70 asphalt ; the telescopic vibrational absorption peaks of ketones C═O (1602.26 cm^{-1}); the telescopic vibrational absorption peaks of sulfinyl S═O (1032.19 cm^{-1}) and the bending vibrational absorption peaks of furan C-H off-surface of substituted benzenes (861.83 cm^{-1}, 808.66 cm^{-1}) in the fingerprint area.

The alkyl telescopic vibrational absorption peaks (2922.89 cm^{-1}, 2852.24 cm^{-1}) and bending vibrational absorption peaks (1457.98 cm^{-1}, 1376.16 cm^{-1}) of rotating film oven-aged asphalt; telescopic vibrational absorption peaks (1576.75 cm^{-1}) of ketones C═O; telescopic vibrational absorption peaks of sulfinyl S═O in the fingerprint region (1025.86 cm^{-1}), carbonyl C═O (945.15 cm^{-1}), and thiophene and pyridine C-H out-of-plane bending vibration absorption peaks (848.76 cm^{-1}, 811.97 cm^{-1}) of substituted benzenes.

The stretching vibration absorption peaks (2922.42 cm^{-1}, 2851.95 cm^{-1}) and bending vibration absorption peaks (1461.25 cm^{-1}, 1376.41 cm^{-1}) of alkyl were obtained by infrared spectrum analysis of PAV (20 h) asphalt. Ketone material C═O stretching vibration absorption peak (1597.63 cm^{-1}); Fingerprint area sulfoxide base S═O stretching vibration absorption peak (1031.95 cm^{-1}) and furan substituted benzene class and pyridine C-H plane bending vibration absorption peak (863.49 cm^{-1}, 755.26 cm^{-1} and 813.74 cm^{-1}).

The IR spectra of PAV (40 h) asphalt were analyzed as follows: C═H stretching vibrational absorption peaks of olefins (3100.36 cm^{-1}); stretching vibrational absorption peaks of alkyl groups (2922.03 cm^{-1}, 2851.32 cm^{-1}) and bending vibrational absorption peaks (1458.43 cm^{-1}, 1376.37 cm^{-1}); stretching vibrational absorption peaks of ketones C═O (1595.39 cm^{-1}); the thiocarbonyl C═S telescopic vibrational absorption peaks (1260.32 cm^{-1}, 1097.06 cm^{-1}, 1018.02 cm^{-1}), the carbonyl C═O telescopic vibrational absorption peaks (944.61 cm^{-1}, 935.85 cm^{-1}), and the substituted benzenes thiophene and pyridine C-H out-of-plane bending vibration absorption peaks (849.11 cm^{-1}, 797.01 cm^{-1}).

From the analysis of FTIR spectra of asphalt at different aging periods, it is clear that the FTIR spectra of asphalt during aging are mainly divided into alkyl region (2923±5 cm^{-1}, 2852±5 cmv, 1460±5 cm^{-1}, 1375±5 cm^{-1}), ketone carbonyl region (1600±5 cm^{-1}), sulfoxide region (1030±5 cm^{-1}) and low fingerprint region (< 1000 cm^{-1}). It can be seen that with the increase of aging time, the area of alkyl region, ketone carbonyl region and sulfoxide region all changed; the peak in the low fingerprint region gradually increased, the peak range gradually became larger, and the stability of the fingerprint region gradually decreased. From the PAV (40 h) aging asphalt spectrum, it can be seen that the chemical structure of the internal mixture has been greatly changed, the original sulfoxide group has been transformed into thiocarbonyl group, a large number of olefins appear, and the peak area of the benzene ring stretching vibration in the fingerprint area has increased sharply.

In order to see more clearly the changes of the peak area of each functional group, the alkyl stretching vibration and bending vibration absorption peak area, ketone carbonyl stretching vibration absorption peak area and sulfoxide group stretching vibration absorption peak area of each asphalt were measured, and the measurement results are shown in Table 4.

Table 4

Area of Vibration Absorption Peak of Alkyl Group

Asphalt samples	70# matrix asphalt	RTFOTL asphalt	PAV (20 h) asphalt	PAV (40 h) asphalt
Alkyl stretching vibration absorption peak (cm-1)	2923.00/ 2852.46	2922.89/ 2852.24	2922.42/ 2851.95	2922.03/ 2851.32
Peak area	3.4939	3.4867	3.4337	3.0459
Alkyl bending vibration absorption Peak (cm-1)	1458.33/ 1376.26	1457.98/ 1376.16	1461.25/ 1376.41	1458.43/ 1376.37
Peak area	1.1435	1.1086	0.9913	0.8681
Stretching Vibration absorption Peak of ketone carbonyl group (cm-1)	1602.26	1576.75	1597.63	1595.39
Peak area	0.1725	0.199	0.2549	0.527
Sulfoxide Stretching Vibration absorption Peak (cm-1)	1032.19	1025.86	1031.95	1260.32/ 1097.06/ 1018.02
Peak area	0.1131	0.1264	0.2345	1.0126

As it can be seen from the data in Table 4, with the increase of asphalt aging, the area of the alkyl region gradually decreases; the area of the ketone carbonyl region and the sulfoxide region gradually increases, the peak area of the alkyl stretching vibration absorption peak gradually decreases, and the peak area of the alkyl bending vibration absorption peak decreases. This indicates that with the deepening of aging two different alkyl absorption peak area change trend, ketone carbonyl absorption peak area and sulfoxide absorption peak area change trend remains the same, and vice versa in the asphalt regeneration process absorption peak area change trend is the same.

4.2.3 FTIR diagram analysis of recycled asphalt

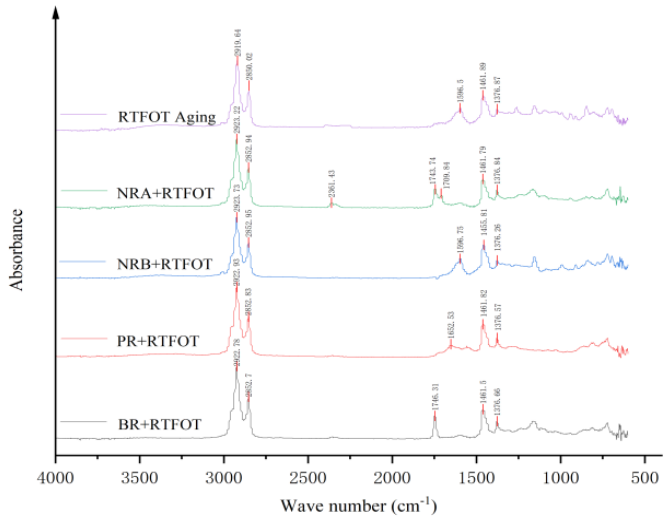

Fig. 8. FTIR Diagram of Reclaimed Asphalt

The test added the RTFOT asphalt specimens without regenerant as a blank control, and thermal aging tests were also conducted. From the test results in Fig. 8, it can be seen that all the four studied samples contain alkyl stretching vibration absorption peaks and bending vibration absorption peaks of single bonds. In addition to the alkyl stretching vibration absorption peak and the bending vibration absorption peak of single bond contained in RTFOT aged asphalt itself, the stretching vibration absorption peak of cyanogenic trigonide (2361.43 cm^{-1}), α-chlorinated non-cyclic ketone vibration absorption peak represented by carbonyl C═O (1743.74 cm^{-1}) and C-O bond stretching vibrational absorption peak (1166.82 cm^{-1}) in lipids. In the NRB recycled asphalt, the vibration absorption peak of carbonyl C═O (1596.75 cm^{-1}) and the vibration absorption peak of C-O bond in lipids (1155.35 cm^{-1}) were observed. The vibrational absorption peaks of carboxylic acid represented by carbonyl C═O (1652.53 cm^{-1}, 1557.99 cm^{-1}) appeared in PR.

The vibrational absorption peaks of α-chlorinated non-cyclic ketones represented by carbonyl C═O (1746.31 cm^{-1}) and the stretching vibrational absorption peaks of C-O bonds in lipids (1159.83 cm^{-1}) appeared in BR. It can be seen that after the addition of the regenerating agent, there is no longer the presence of sulfoxide group in the asphalt spectrum after the second aging, and the peak of carbonyl group also changed, indicating that the original compound structure of carbonyl group and sulfoxide group has been reorganized or dispersed away. The peak areas of the regenerated asphalt spectra after the addition of NRA, NRB, PR, and BR were 0.7567, 0.6228, 0.6345, and 0.4429, indicating that all four regenerants can effectively reduce the generation of sulfoxide groups, with BR being the best, NRB and PR the second best, and NRA the worse for preventing the generation of carbonyl groups.

In order to show the regeneration effect of the regenerant more visually, the regeneration effect was measured by the change of peak area. The addition of the regenerant's own components will have an effect on the functional group analysis, and the change in the peak area of the sulfoxide and carbonyl indices and the change in the combination of functional groups make it impossible to quantitatively analyze the sulfoxide and carbonyl indices. However, the four regenerants and RTFOT aging asphalt analyzed in the study all contain alkyl stretching and single bond bending vibration absorption peaks, and the peak and functional group did not change substantially, so the alkyl change index is defined as expressed by Eq:

$$I_a = \frac{A_{ia} - A_a}{A_a} \tag{1}$$

$$I_b = \frac{A_{ib} - A_b}{A_b} \tag{2}$$

$$I = I_a + I_b \tag{3}$$

I is alkyl change index; I_a is the stretching vibration index; I_b is the bending vibration index; Aa is the alkyl stretching vibration absorption peak area of RTFOT aging asphalt; Ab is the bending vibration absorption peak area of alkyl single bond of RTFOT aged asphalt. Aia is the alkyl stretching vibration absorption peak area of NRA, NRB, PR and BR reclaimed asphalt, respectively. Aib is the alkyl single bond bending vibration absorption peak area of NRA, NRB, PR and BR reclaimed asphalt respectively. The peak area is calculated by OMNIC software and calculated according to equations (1), (2) and (3). The analysis results are shown in Table 5.

Table 5

Alkyl Index

Type of regenerator used	NRA	NRB	PR	BR
Stretching vibration index Ia	0.1621	0.0137	0.1902	0.1992
Bending vibration index Ib	0.0308	0.2970	0.0240	0.1744
Alkyl change index I	0.1929	0.3107	0.2142	0.3737

From Table 5, it can be seen that NRB is less effective in improving the telescopic vibration index, NRA and PR are not effective in improving the bending vibration index, and only BR has a good improvement in both telescopic and bending vibration indices. Although the penetration rate of NRA was the fastest in the needle penetration model test, the regeneration effect of alkyl change index was not good, which was probably due to the excessive light components in NRA, as evidenced by its dynamic viscosity of 53.6 mm²/S at 60 ℃ and density (25 ℃) of 0.91 g/cm² can be seen that it mainly relies on the molecular Brownian motion of the light components to achieve a better permeation effect. NRB, on the other hand, adds a colloidal component to NRA, which can be seen to have a significant effect on the alkyl bending vibration index. However, the effect of PR is very similar to that of NRA, but the penetration ability of PR is not very good, which indicates that the regeneration components are not complete or the light components are not enough, and the relevant colloidal components are also missing.

5. Conclusions

The permeability and regeneration performance of four regenerators NRA, NRB, PR and BR were analyzed by penetration degree and Fourier infrared spectroscopy test. The peak value and peak area changes of functional groups in FTIR spectra were deeply studied, and the osmotic regeneration mechanism of regenerators was comprehensively analyzed. The main conclusions were as follows:

(1) In the penetration degree test of the penetration model with different time, temperature, type and dosage of regenerating agent, four kinds of change graphs were obtained, namely: concave graph, convex graph, rising graph and waveform graph, and the penetration effect of regenerating agent was determined as NRA > NRB > PR > BR. The infiltration ability of NRA and NRB is strong, and the optimum content is about 5% and 10%, respectively. The high temperature stability of PR is good, while the permeability of BR is relatively poor.

(2) With the increase of asphalt aging degree, the absorption peak areas of carbonyl group and sulfoxide group gradually increase, and the peak areas of alkyl stretching vibration absorption peak and alkyl bending vibration absorption peak gradually decrease. Two different alkyl absorption peaks with aging the regeneration effect can be indirectly judged by the alkyl absorption peak area in the FTIR profile of asphalt.

(3) All the four regenerating agents can effectively prevent the formation of sulfoxide group. BR has the best effect on limiting the formation of carbonyl group, followed by NRB and PR, and NRA is poor. According to the alkyl stretching vibration absorption peak and bending vibration absorption peak, the alkyl change index result is BR > NRB > PR > NRA. The results indicated that the regeneration effect of the regenerator was BR > NRB > PR > NRA.

(4) There is a certain difference between the results of infiltration velocity and regeneration effect obtained from the infiltration interlayer model. The main reason is that there is too much content of light components in the non-petroleum-based regeneration agent and the density gap is too large, which only shows the infiltration effect but does not play a good regeneration effect. Therefore, the permeation effect and regeneration effect of regenerating agent should be considered comprehensively for the practicability of regenerating agent.

(5) Based on the penetration of regenerant and regeneration penetration mechanism, the regeneration process of comprehensive evaluation of regenerant content is only a rough analysis, in subsequent studies need to put the regenerant dosage in-depth variable analysis, explore and combination of asphalt mixture, thus further validation regenerant penetration mechanism.

Acknowledgments

This work was financially supported by the Science and Technology Fund Project of Jiangxi Provincial Transportation Department(2022H0009) and the Science and Technology Fund Project of Jiangxi Provincial Transportation Department (2023H0024).

R E F E R E N C E S

[1]. Mivehchi M; Wen HF; Wen YK; Wang L. Study of Measures to Design Asphalt Mixes Including High Percentages of Recycled Asphalt Pavement and Recycled Asphalt Shingles. Transportations Research Record, 2022.2(2677):869-879.

[2]. Kumar Ankush; Choudhary Rajan; Kumar Abhinay. Storage stability performance of composite modified asphalt with scrap non-tire automotive rubber, waste plastic pyrolytic oil and sulfur. PLoS ONE, 2023.4(17):1-23.

[3]. Hoy M ; Samrandee V; Samrandee W, et al. Evaluation of asphalt pavement maintenance using recycled asphalt pavement with asphalt binders. Construction and Building Materials, 2023(406).

[4]. ZHAO Xinyu/ LIU Xueting. Influence analysis of permeable regenerating agent on performance of aging asphalt. Highway & Automobile Transportation, 2017(03): 76-79.

[5]. Pouget S; Marsac P; Pedraza A; Sauzéat C; Di Benedetto H; Gaudefroy V; Boulangé L; Pévère A; Mouillet V. Advanced characterisation of multi-recycled warm asphalt pavement (MRWAP) with high content of recycled asphalt pavement. Road Materials and Pavement Design, 2021.2(24):388-409.

[6]. ELEYEDATH A/SWAMY A K. Use of waste engine oil in materials containing asphaltic components. London: Ecoefficient Pavement Construction Materials, 2020

[7]. CHEN Huaxin, CUI Yu, YIN Yanping, et al. Effect of type of reactivator on antiaging pr-operty of asphalt. China Science and Technology Paper, 2021, 17(06): 589-594.
[8]. Jain S; Chandrappa AK. Critical review on waste cooking oil rejuvenation in asphalt mixture with high recycled asphalt. Environmental Scienceand Pollution Research, 2023.32(30):77981-78003.
[9]. Izaks R; Gebauere L; Sparans R; Kornisovs R; Haritonovs V. Use of recycled asphalt and waste materials in production of high performance asphalt mixtures. Baltic Journal of Road and Bridge Engineering, 2022.4(17):120-145.
[10]. WU Jianjun, YANG Zhe, ZHANG Hongbing, et al. Evaluation of road performance of permeable regenerating agent for regenerating aging asphalt mixture. Shanxi Transportation Science and Technology, 2021(06): 4-9.
[11]. Kaseer F; Arámbula-Mercado E ; Cucalon LG; Martin AE. Performance of asphalt mixtures with high recycled materials content and recycling agents. International Journal of Pavement Engineering, 2020.7(21):863-877.
[12]. Büchner J; Wistuba MP. Assessing creep properties of asphalt binder, asphalt mastic and asphalt mixture. Road Materialsand Pavement Design, 2022.S1(23):116-130.
[13]. Barghabany P; Zhang J; Mohammad LN; Cooper SB. Chemical and Rheological Characterization of Asphalt Binders: A Comparison of Asphalt Binder Aging and Asphalt Mixture Aging. Transportations Research Record, 2022.5(2676):147-157.
[14]. WU LAN, ZHAO Kehong, ZHANG Guohong. Characterization of recycled asphalt based on microanalysis. Chinese journal of ceramics, 2018, 37(11): 3684-3689.
[15]. Sharma A; Ransinchung RNGD ; Kumar P. Applicability of various mixing rules for hot asphalt recycled binders. Road Materials and Pavement Design, 2021.11(23):2547-2566.
[16]. CHEN Long, CHEN Hongbin, LI Peng, et al. Evaluation of interfacial wetting and diffusion fusion performance of regenerant and waste asphalt. Highway, 2021, 66(10): 1-9.
[17]. Riccardi C; Falchetto AC; Losa M ; Wistuba MP. Rheological modeling of asphalt binder and asphalt mortar containing recycled asphalt material. Materials and Structions, 2016(49):4167-4183.
[18]. WANG Lei/ZHANG Shuxian. Study on low temperature performance and micro mechanism of asphalt aging regeneration. Inner Mongolia Highway and Transportation,2022(03): 14-17.
[19]. Elkashef Mohamed; Williams R. Christopher; Cochran Eric. Thermal stability and evolved gas analysis of rejuvenated reclaimed asphalt pavement (RAP) bitumen using thermogravimetric analysis–Fourier transform infrared (TG–FTIR). Journal of Thermal Analysis & Calorimetry, 2018.2(131):865-871.
[20]. WANG, Fusong, ZIPENG Wang, CHAO Li, et al. The rejuvenating effect in hot asphalt recycling by mortar transfer ratio and image analysis. Materials 2017, 10.
[21]. Li. Study on diffusion behavior of asphalt regenerating agent and its influencing fact-ors. China University of Petroleum, 2010.
[22]. XIAO Qingyi, ZHANG Mengqi, ZHANG Jingjie. Mechanism and influencing factors of permeable regeneration of regenerating agents. Journal of Hebei university of technology, 2017, 46(04): 85-91.
[23]. XU Meng/QUAN Dong. Analysis of regeneration agent diffusion process based on Fick's Law. // Academic Proceedings of Jiangsu Highway Society (2017), 2018: 80-86.
[24]. ZHAN Congming, CHEN Xiang, GUAN Yongsheng, et al. Diffusion behavior and performance evaluation of high efficiency regenerant. Heilongjiang science, 2018, 9(22): 16-18.
[25]. FORTON A., DI Benedetto H., Mangiafico, et al. Rheological properties of fresh and RAP bitumen blends with or without regenerating agent. Bituminous Mixtures and Pavements VII, 2019.

[26]. XU Jinzhi, ZHANG Binyan, ZHANG Depeng. Regeneration of aged asphalt based on diffusion behavior of regenerant/new asphalt. Bulletin of the Chinese Ceramic Society, 2021, 40(12): 4187-4196.
[27]. Cui Shuyu. Properties and diffusion mechanism of recycled asphalt in complex environment. Inner Mongolia University of Technology, 2021.